Gem-Quality Anorthoclase Feldspar From Southeast Vietnam

Le Ngoc Nang, Pham Minh Tien, Pham Minh, and Pham Trung Hieu

In southeast Vietnam, gem-quality anorthoclase is found as megacrysts in Cenozoic alkali basalt. The crystals are transparent to translucent with vitreous luster and can be near-colorless, yellow, or brownish gray. Gemological testing confirmed this mineral is alkali feldspar, but the data cannot specify the alkali feldspar subgroup (orthoclase, anorthoclase, microcline, or sanidine). Based on X-ray diffraction analysis and a feldspar composition ternary diagram created from energy-dispersive X-ray fluorescence analysis, this material was identified as anorthoclase. Energy-dispersive X-ray fluorescence determined the composition to be $An_{3.50–8.02}$, $Ab_{58.83–81.69}$, and $Or_{11.94–36.96}$. The Raman spectra displayed differences when compared to those of other alkali feldspars such as sanidine, orthoclase, and microcline. Fourier-transform infrared spectra of this material are similar to those of anorthoclase from around the world and lack any distinctive features that would allow for its separation. Gem-quality anorthoclase from southeast Vietnam has commercial potential, as it is abundant and evenly distributed in the basaltic weathering products.

The feldspar group of minerals are rock-forming aluminum tectosilicates that include a wide range of well-known gemstone varieties such as moonstone (orthoclase), sunstone, labradorite (plagioclase), and amazonite (microcline) (Bonewitz, 2008). Alkali feldspar is a subgroup that ranges between sodium-rich feldspar ($NaAlSi_3O_8$) and potassium-rich feldspar ($KAlSi_3O_8$) and includes the monoclinic varieties sanidine and orthoclase as well as the triclinic varieties anorthoclase, albite, and microcline (Deer et al., 2001; Bonewitz, 2008). Variety classification is not possible using standard gemological methods because of overlapping properties such as specific gravity (SG), refractive index (RI), optic figure, fluorescence reaction, and absorption spectrum in the visible region. However, each of these varieties has distinct crystallographic structures, making it possible to identify them using X-ray diffraction methods (Harlow, 1982). Chemical composition also plays a vital role in establishing the alkali feldspar variety.

Anorthoclase, $(Na,K)AlSi_3O_8$, is an uncommon variety of alkali feldspar that is the potassium-rich variety of high albite, distinguished from sanidine by its triclinic symmetry (Jones and Taylor, 1961; Bendel and Schmidt, 2008). The entire solid solution between high albite and sanidine can form at high temperature. The color palette ranges from near-colorless to yellow and brownish gray (figure 1). Anorthoclase has a Mohs hardness of 6.5 and is characterized by albite-law twinning with perfect cleavage in two directions (Anthony et al., 2001). It is rarely used in the jewelry industry.

In Brief

- The feldspar species anorthoclase has been found in southeast Vietnam, originating from Cenozoic alkali basalt.
- The Vietnamese anorthoclase crystals studied here are yellow, brownish gray, or near-colorless, with a transparent to translucent appearance and vitreous luster, and sometimes they display chatoyancy and asterism.
- FTIR, Raman, and XRD spectroscopy, together with standard gemological properties, can confirm the anorthoclase variety (potassium-rich albite).
- Vietnamese anorthoclase is suitable for cutting into faceted and cabochon gems for use in jewelry.

In the Cenozoic alkali basalt of southeast Vietnam, anorthoclase megacrysts are enclosed in the host rock or scattered in the soil formed from basaltic weathering. These megacrysts are concentrated on ancient volcanic slopes that are currently used for farming. Previous studies have reported on the exis-

See end of article for About the Authors and Acknowledgments.
Gems & Gemology, Vol. 60, No. 2, pp. 194–207,
http://dx.doi.org/10.5741/GEMS.60.2.194

Figure 1. Yellow, brownish gray, and near-colorless anorthoclase feldspar from southeast Vietnam. The rough stones range from 96.5 to 144.8 ct and the cut samples from 3.64 to 11.07 ct. Photos by Le Ngoc Nang.

tence of anorthoclase in the region but with very limited descriptions, especially with regard to its gemological properties (Hoang and Flower, 1998). Earlier authors only categorized their samples as alkali feldspar without specifying the variety, as no structural and chemical composition analyses were performed at the time.

To date, anorthoclase has yet to be applied in the jewelry industry. Nang and Tien (2021) first recorded gem-quality anorthoclase in Dong Nai Province of southeast Vietnam. The article also reported two translucent samples that displayed chatoyancy and sheen effects. Although anorthoclase has received little attention in the past, we believe there is potential economic value in the gem-quality material from Dong Nai. This paper aims to provide new data on samples to identify the alkali feldspar variety and characterize this material in order to assess its gem quality and commercial potential.

GEOLOGICAL SETTING

Vietnam experienced two primary tectonic events. The first was the Indosinian orogeny during the Triassic (250–240 Ma). This resulted from the tectonic collision between the Indochina Plate and the Yangtze Plate, which lifted the northwest portion of the Indochina block toward the adjacent continents originating from the Gondwana supercontinent (Carter et al., 2001; Lepvrier et al., 2008). The second occurred when the Indian Plate collided with the Eurasian Plate in the Paleogene (50–55 Ma) (Clift et al., 2002; Leech et al., 2005). The large-scale basaltic eruptions along the eastern and southeastern coast of Asia, including the West Pacific offshore, played a fundamental role in regional geology (Barr and MacDonald, 1981). The eruptions consisted of several basaltic phases, later forming structures separated by faults and developed mainly in east Indochina, including southeast Vietnam (Rangin et al., 1995).

Southeast Vietnam has a total area of 23,000 km^2, and approximately 10,000 km^2 is covered by basaltic formations with thicknesses ranging from a few meters to over a hundred meters (figure 2) (Hoang and Flower, 1998). Two periods of magmatic eruption have been recorded in the region. The first eruption, dating 8 Ma to the Neogene, included quartz and olivine tholeiitic magmatic series. This was followed by olivine tholeiite, alkali basalt, and basalt in the second eruption, during the Quaternary (Hoang et al., 1996; Tich et al., 2004). The quartz and olivine tholeiitic magmatic series consists of basalt, two-pyroxene basalt, dolerite basalt, and olivine-poor hyalobasalt. These have massive and vesicular structure, black to gray color, and a low potassium content of <1% (Hoang et al., 1996). The series of olivine tholeiite, alkali basalt, and basalt contains xenoliths that may be associated with gemstones, as well as individual megacrysts such as garnet, zircon, augite, corundum, peridot, and feldspar.

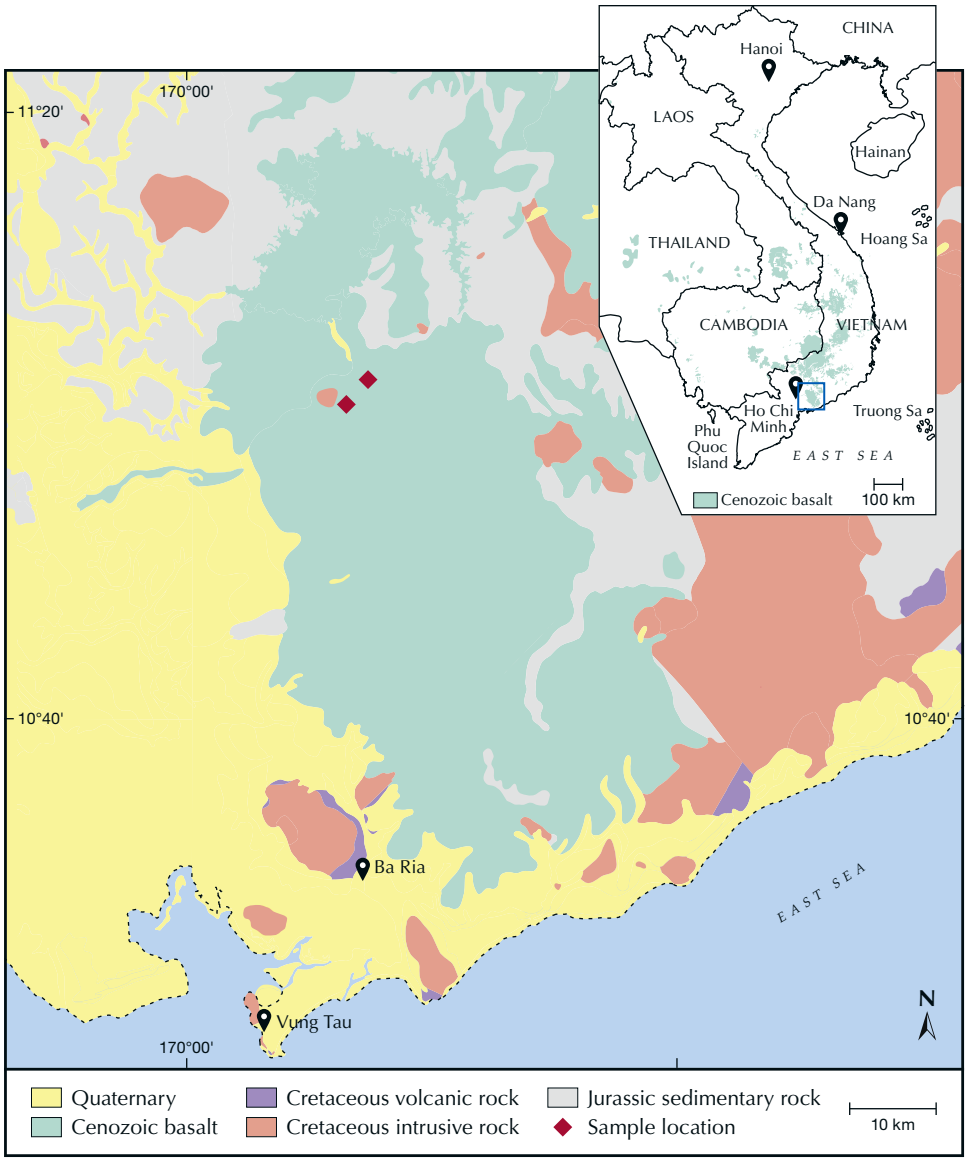

Figure 2. Geological map of southeast Vietnam. Anorthoclase is found in the middle of Cenozoic basalt. From Son (2005), modified by Le Ngoc Nang.

The anorthoclase in this study occurs as megacrysts within the alkali basalt. Weathering of these basaltic layers made it easier to access the anorthoclase (figure 3; visit https://www.gia.edu/gems-gemology/summer-2024-anorthoclase-feldspar).

MATERIALS AND METHODS

Samples. A total of 96 samples were obtained from two locations (see figure 2) in 2020 and 2022. They ranged from 5 to 1550 ct and consisted of 65 near-colorless, 17 brownish gray, and 14 yellow pieces (author LNN collected 34 samples, and 62 were provided by locals). Of the 96 samples, 33 were selected for faceting and cabochon cutting. We chose 14 rough specimens weighing over 6 ct in all available colors (near-colorless, brownish gray, and yellow), two transparency levels (transparent and translucent, including some chatoyant and four-rayed star samples; visit https://www.gia.edu/gems-gemology/summer-2024-anorthoclase-feldspar), most with good clarity. These were used to establish gemological properties, chemical composition, and spectroscopic features. The 14 samples consisted of eight faceted stones (AF1–AF8), two cabochons (AF9–AF10), and four rough samples (AF11–AF14) (figure 4). The faceted and cabochon specimens were cut by Nguyen Tri Duc, an expert cutter working in collaboration with Liu Gemological Research and Application Center (LIULAB) in Ho Chi Minh City. In addition, portions of samples AF12 (yel-

Figure 3. Nodules of anorthoclase were discovered in massive basalt by the lead author in sizes up to 22 cm (A), 6 cm in vesicular basalt (B), and 4 cm as fragments in alluvial deposits (C). Photos by Pham Minh Tien.

low), AF14 (near-colorless), and AF9 (brownish gray; the leftover material from cutting) were ground to powder for X-ray diffraction (XRD) analysis.

Methods. *Standard Gemological Testing*. Standard gemological testing was performed at LIULAB. The physical appearance of the samples was observed under a 60W GLS LED daylight bulb with a light temperature of approximately 5000–6000K. The SG of all 14 samples was measured using the hydrostatic method. A refractometer with a sodium light source and an optical coupling liquid of methylene iodide and

Figure 4. Anorthoclase samples from this study consisted of eight faceted stones, two cabochons, and four rough samples within three color groups: near-colorless, brownish gray, and yellow. Photos by Le Ngoc Nang.

tetraiodoethylene (RI of 1.81) was employed to measure the refractive index of the cut stones (AF1–AF10). Optical properties and pleochroism of high-transparency gems were observed using a polariscope and a dichroscope, respectively. All samples were exposed to ultraviolet light to determine their fluorescence reaction to long-wave (365 nm) and short-wave (254 nm) UV. A scratch test was performed to determine Mohs hardness. A Carton SPZV50 gemological microscope was used to view the internal features of the cut samples (AF1–AF10), with a magnification of 7× to 50×.

X-Ray Diffraction (XRD). Samples AF9, AF12, and AF14 were exposed to incident X-ray radiation to determine their crystallographic structures, which defines the variety of feldspar for each. The technique was performed using a Bruker D2 Phaser benchtop X-ray powder diffractometer, with Cu Kα radiation in the range of 5–75° 2θ with a scan speed of 0.02°/s, at 40 kV and 30 mA. The analyzed data were interpreted using X'Pert Highscore Plus software, which compared the analyzed results to the standard data in the Inorganic Crystal Structure Database (ICSD; Levin, 2018). XRD was conducted on near-colorless, yellow, and brownish gray powdered samples, with an average particle size of about 0.05 mm. These were processed and analyzed at the Institute of Chemical Technology, Vietnam Academy of Science and Technology in Ho Chi Minh City.

Energy-Dispersive X-Ray Fluorescence (EDXRF). We analyzed 14 samples (AF1–AF14) using a Shimadzu EDX-8100 operated with a voltage of 30 kV and a current of 10 mA. The reference standards for Al_2O_3, SiO_2, TiO_2, MgO, MnO, FeO, Na_2O, CaO, K_2O, and Cr_2O_3 were corundum, quartz, titanium dioxide, periclase, manganosite, fayalite, jadeite, wollastonite, potassium titanium phosphate, and eskolaite, respectively. The detection limits were calculated based on the system of Glascock (2020): 0.02 wt.% for Al_2O_3 and SiO_2; 0.01 wt.% for MgO and Na_2O; and 0.0002 wt.% for TiO_2, MnO, FeO, CaO, K_2O, and Cr_2O_3. EDXRF was conducted at the Center of Analytical Services and Experimentation in Ho Chi Minh City.

Raman Spectroscopy. A Horiba Xplora One was employed to obtain the Raman spectra in the 0–3750 cm^{-1} range for samples AF1, AF3, and AF7. Measurements were performed at a laser excitation wavelength of 532 nm, laser mode power at 50%, and 900 lines/mm diffraction grating, with a spectral resolution of 5 cm^{-1}. The objective selected was of 50× magnification. Raman spectra were collected over 15 s with two signal accumulations. The analysis was conducted at the Institute of Chemical Technology, Vietnam Academy of Science and Technology.

Fourier-Transform Infrared (FTIR) Spectroscopy. A Cary 630 FTIR instrument with attenuated total reflection (ATR) was used to efficiently collect the FTIR spectra of samples AF1, AF2, and AF7. Measurements were obtained in a spectral range of 4000–400 cm^{-1} with a resolution of <2 cm^{-1} and a scanning time of 3 s. The analysis was performed at LIULAB.

RESULTS AND DISCUSSION

Appearance. From the total of 96 samples collected during field trips, three colors were noted: near-colorless, brownish gray, and yellow (figures 1 and 4). Near-colorless samples were most common, followed by brownish gray, while yellow was comparatively rare. The majority of the gems collected were transparent to semitransparent; a few were translucent, and opaque samples were also found but rarely used because of their poor quality (figures 1 and 4; table 1). These materials were subhedral and anhedral fragments with good cleavage and conchoidal fracture. Some specimens bore etch marks on the surface due to surface corrosion. The samples showed vitreous luster. The yellow and brownish gray samples accounted for 5% and 7% of all of the collected samples, respectively. They had better clarity and transparency than the near-colorless samples, with few feathers along the cleavage. However, the brownish gray samples had lower clarity (i.e., a more cloudy appearance) than the yellow samples. The yellow and brownish gray stones were easier to cut than the near-colorless samples, which often developed deep cracks along the cleavage. Among the translucent samples, we encountered an anorthoclase with a cat's-eye effect (Nang and Tien, 2021).

Gemological Properties. The refractive indices measured on eight faceted stones (AF1–AF8) were n_α = 1.518–1.523 and n_γ = 1.526–1.531, with a birefringence of 0.007–0.008. The specific gravity of 14 samples determined by the hydrostatic method ranged from 2.59 to 2.62 (table 1). The Mohs hardness of the rough anorthoclase was 6.0–6.5. These properties were consistent with alkali feldspar (Bonewitz, 2008) but cannot help distinguish between orthoclase, microcline, sanidine, albite, and anorthoclase.

TABLE 1. Gemological properties of anorthoclase from Dong Nai, Vietnam.

Sample no.	Color	Form	Transparency	Weight (ct)	SG	RI (birefringence)	Fluorescence reaction
AF1	Light yellow	Faceted cushion	Transparent	25.99	2.61	1.520–1.528 (0.008)	Long-wave: Inert Short-wave: Weak pink
AF2	Yellow	Faceted oval	Transparent	12.24	2.59	1.518–1.525 (0.007)	Inert to long-wave and short-wave
AF3	Brownish gray	Faceted octagon	Transparent	10.95	2.61	1.520–1.528 (0.008)	Inert to long-wave and short-wave
AF4	Yellow	Faceted rectangle	Transparent	3.81	2.60	1.518–1.526 (0.008)	Inert to long-wave and short-wave
AF5	Yellow	Faceted oval	Transparent	11.07	2.61	1.520–1.528 (0.008)	Inert to long-wave and short-wave
AF6	Light yellow	Faceted lozenge	Transparent	4.67	2.60	1.517–1.525 (0.007)	Inert to long-wave and short-wave
AF7	Near-colorless	Faceted round	Transparent	3.64	2.62	1.523–1.531 (0.008)	Inert to long-wave and short-wave
AF8	Near-colorless	Faceted trilliant	Transparent	1.48	2.61	1.520–1.527 (0.007)	Inert to long-wave and short-wave
AF9	Brownish gray	Round cabochon	Translucent	3.27	2.61	1.52[a]	Inert to long-wave and short-wave
AF10	Brownish gray	Oval cabochon	Translucent	7.50	2.60	1.52[a]	Inert to long-wave and short-wave
AF11	Grayish yellow	Rough	Transparent	144.80	2.60	n/a	Inert to long-wave and short-wave
AF12	Grayish yellow	Rough	Transparent	54.90	2.60	n/a	Inert to long-wave and short-wave
AF13	Very light yellow	Rough	Transparent	37.28	2.69	n/a	Inert to long-wave and short-wave
AF14	Near-colorless	Rough	Transparent	52.60	2.59	n/a	Long-wave: Inert Short-wave: Weak pink

[a]*Measured using a spot reading method*

Twelve of the 14 samples were inert under UV light, while the other two (AF1 and AF14) emitted weak pink fluorescence under short-wave UV light. This differs from some alkali feldspars such as plagioclase and orthoclase, which fluoresce red or pink to long-wave UV (Morrison and Cox, 2014). Transparent samples displayed a biaxial pattern under the polariscope and did not show pleochroism. These features have been observed in more than one variety of alkali feldspar, with no clearly defined boundaries to distinguish them based on gemological properties.

Hence, the samples' appearance and gemological properties confirmed these were all alkali feldspars but could not differentiate which varieties they were.

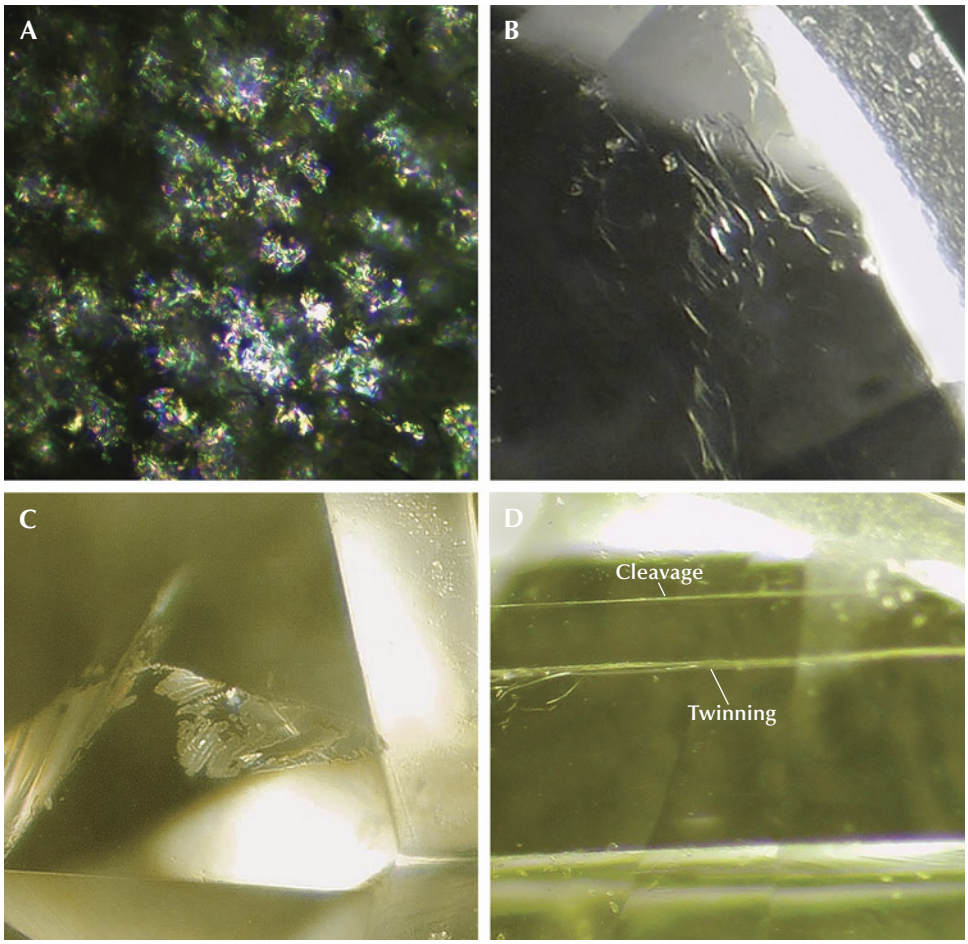

Figure 5. Inclusions in anorthoclase from southeast Vietnam. A: A myriad of incomplete thin, flat fluid inclusions reflecting interference colors (sample AF9). B: Worm-like fluid inclusions (sample AF7). C: Colorless healed fractures along the cleavage (sample AF5). D: Cleavage planes accompanied by albite-law twinning, identified using a polariscope (sample AF4). Photomicrographs by Le Ngoc Nang; fields of view 1.8 mm (A) and 2.5 mm (B–D).

Internal Features. Examining the cut gems, we detected fluid inclusions, healed fractures, cleavage planes, and twinning planes (twinning and cleavage planes were distinguished with a polariscope) (figure 5). Tiny fluid inclusions formed incomplete reflective and flat thin films that were directionally distributed in most near-colorless and brownish gray samples (figure 5A, sample AF9). Worm-like fluid inclusions were found in two samples (e.g., figure 5B, sample AF7), and these grew along the plane identified as albite-law twinning using a polariscope. Healing of fractures, which formed during rapid cooling from high temperature (Gübelin and Koivula, 2005), was observed in samples AF1–AF7, developing along the cleavages of the feldspar host (figure 5C, sample AF5). Characteristic perfect cleavage was observed in most of the samples along with the albite-law twin planes, as seen in figure 5D (sample AF4). Unfortunately, we could not determine the fluid inclusions by Raman analysis.

X-Ray Diffraction. While standard gemological testing methods are not effective for distinguishing alkali feldspar varieties, XRD can separate them based on their different crystal structures. Our XRD analyses for three samples (near-colorless, yellow, and brownish gray) from southeast Vietnam were consistent with the anorthoclase sample 01-075-1630 from the ICSD database (Levin, 2018) (figure 6). This result helped us confirm that the samples in all three colors were anorthoclase.

Chemical Composition. The chemical composition of 14 anorthoclase specimens determined with EDXRF is shown in table 2, in which Al_2O_3 ranges from 17.82 to 25.94 wt.%, SiO_2 from 60.10 to 67.12 wt.%, CaO from 0.64 to 1.51 wt.%, Na_2O from 5.90 to 9.52 wt.%, and K_2O from 2.15 to 6.13 wt.%. The concentration of main oxides, especially sodium and potassium, varied from sample to sample. In all measured samples, the sodium concentrations were higher than those for potassium. The transition from anorthoclase to sanidine occurs during the replacement of sodium by potassium, accompanied by increasing structural disorder. The K/(K+Na) in our

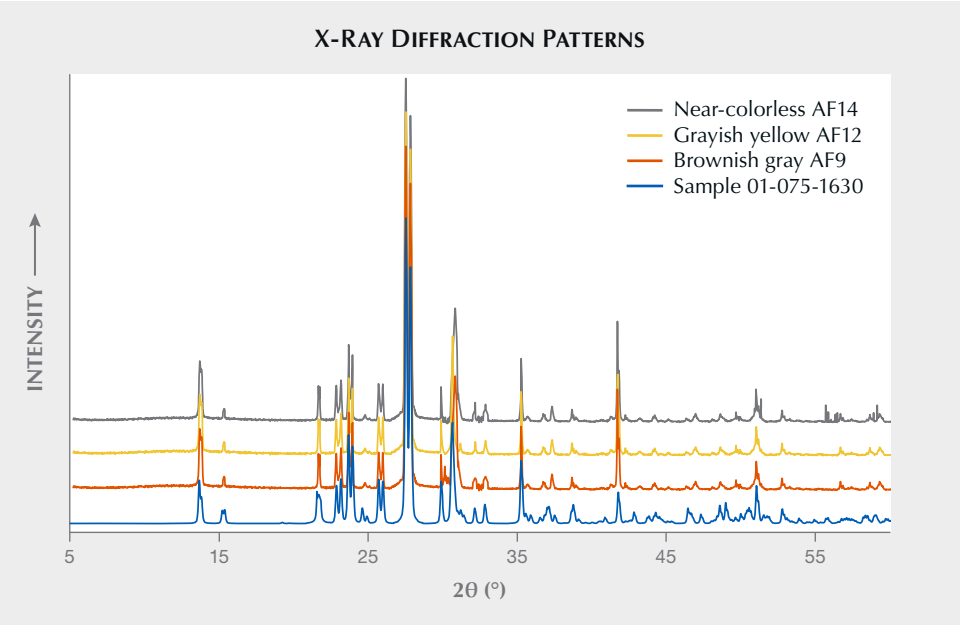

Figure 6. X-ray diffraction patterns of anorthoclase samples from southeast Vietnam and an ICSD reference sample included for comparison. Spectra are offset vertically for clarity.

samples ranged between 0.12 and 0.38, corresponding to anorthoclase rather than sanidine (Bendel and Schmidt, 2008). In addition, we noted a low calcium content (0.031–0.073) that corresponded with potassium-rich albite instead of calcium-potassium-rich albite (where the albite is more enriched in calcium than potassium). Meanwhile, we also determined there were very minor amounts of the trace elements iron, magnesium, titanium, and manganese. We calculated the following ratios: anorthite (An) 3.50–8.02%, albite (Ab) 58.83–81.69%, and orthoclase (Or) 11.94–36.96%. In all, 13 of the 14 samples fell within the anorthoclase (potassium-rich albite) region, and one sample (AF6) belonged to the albite field on the plotted An-Ab-Or system (figure 7).

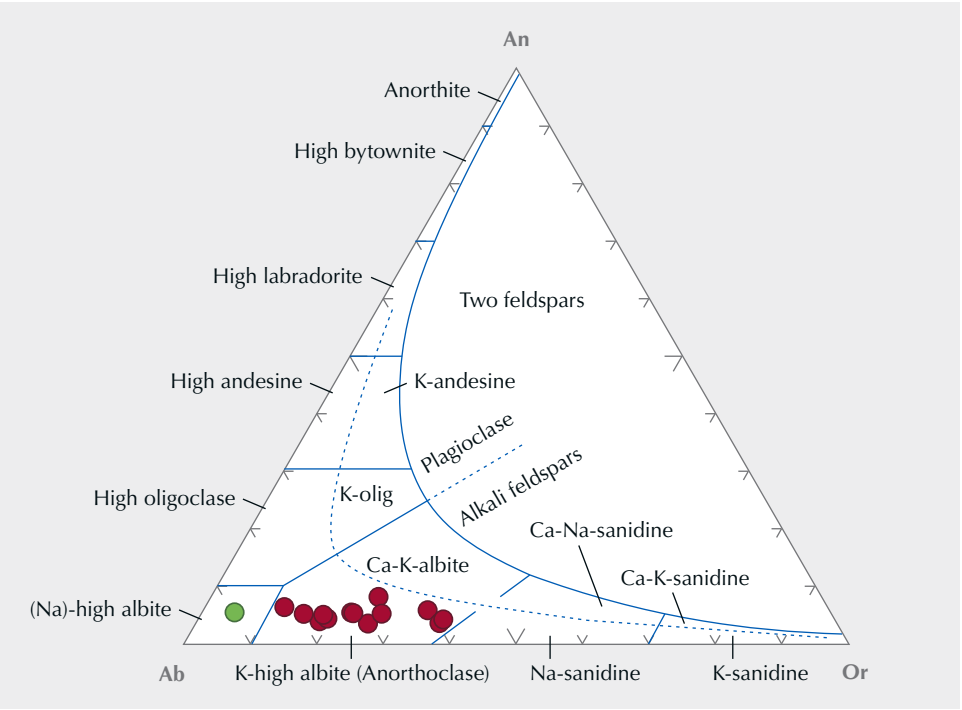

Figure 7. In the An-Ab-Or (anorthite-albite-orthoclase) composition diagram, all but one of the samples are concentrated in the range of anorthoclase (potassium-rich albite) (Smith and Brown, 1988). Note that the green dot corresponds to sample AF6.

TABLE 2. Chemical composition of anorthoclase from Dong Nai, Vietnam, obtained by EDXRF.

	AF1	AF2	AF3	AF4	AF5	AF6	AF7	AF8	AF9	AF10	AF11	AF12	AF13	AF14
Oxide (wt.%)														
SiO_2	63.96	63.57	65.54	66.14	61.13	67.12	60.10	63.45	62.78	66.55	65.05	64.35	66.01	67.10
TiO_2	0.01	bdl[b]	bdl	0.01	0.02	bdl	0.01	bdl	bdl	bdl	bdl	bdl	bdl	bdl
Al_2O_3	22.90	23.01	20.54	19.04	25.94	18.94	25.74	23.70	22.80	19.19	20.89	21.47	20.12	17.82
FeO[a]	0.77	0.61	0.56	0.46	0.557	0.46	0.65	0.65	0.81	0.32	0.03	0.39	0.47	0.55
MnO	bdl	bdl	bdl	bdl	bdl	bdl	bdl	bdl	bdl	bdl	bdl	bdl	bdl	bdl
MgO	0.12	0.50	0.39	0.46	0.60	0.35	0.50	0.32	0.72	0.41	0.22	0.40	0.53	0.42
CaO	0.76	0.83	1.09	1.19	0.91	1.34	0.64	0.97	1.51	0.73	0.77	0.83	1.06	1.10
Na_2O	8.35	8.03	8.03	6.83	7.65	9.52	5.90	8.20	6.99	8.11	7.01	6.42	7.92	7.90
K_2O	3.02	3.10	3.84	5.81	2.82	2.15	5.51	2.43	3.92	4.57	5.44	6.13	3.83	4.83
Atoms per formula unit, 8 O (charge balance)														
Si	2.839	2.828	2.916	2.964	2.719	2.973	2.706	2.821	2.813	2.962	2.915	2.879	2.939	3.000
Al	1.198	1.207	1.077	1.005	1.359	0.988	1.375	1.242	1.204	1.007	1.103	1.133	1.056	0.939
Fe^{2+}	0.022	0.020	0.020	0.017	—	0.012	0.021	0.024	0.030	0.080	0.011	—	0.018	0.021
Fe^{3+}	0.006	0.003	—	—	0.021	0.005	0.004	—	—	0.004	—	0.013	—	—
Mg	0.008	0.033	0.026	0.031	0.039	0.023	0.034	0.021	0.048	0.027	0.015	0.027	0.035	0.028
Ca	0.036	0.040	0.052	0.057	0.043	0.064	0.031	0.046	0.073	0.035	0.037	0.040	0.051	0.053
Na	0.718	0.693	0.692	0.593	0.659	0.815	0.515	0.707	0.607	0.700	0.609	0.557	0.684	0.685
K	0.171	0.177	0.216	0.332	0.159	0.119	0.316	0.138	0.224	0.258	0.311	0.350	0.218	0.275
K/(K+Na)	0.192	0.203	0.238	0.360	0.194	0.127	0.380	0.163	0.270	0.269	0.338	0.386	0.242	0.286
Ternary system of anorthite-albite-orthoclase														
An	3.91	4.35	5.41	5.81	5.028	6.37	3.58	5.19	8.02	3.50	3.86	4.20	5.31	5.20
Ab	77.62	76.22	72.09	60.39	76.49	81.69	59.72	79.34	67.19	70.52	63.64	58.83	71.83	67.60
Or	18.47	19.43	22.50	33.80	18.49	11.94	36.69	15.47	24.79	25.97	32.49	36.96	22.86	27.19

[a]*FeO = total iron*
[b]*bdl = below detection limit. Detection limits = SiO_2 and Al_2O_3: 0.002; TiO_2, FeO, MnO, and CaO: 0.0002; MgO and Na_2O: 0.01; and K_2O: 0.001.*

Raman Spectroscopy. Raman and FTIR spectra were measured on three faceted anorthoclase samples with different colors: light yellow (AF1), brownish gray (AF3), and near-colorless (AF7). In the 100–600 cm^{-1} range, the samples displayed four strong peaks at 165, 283, 476, and 510 cm^{-1} (figure 8). These peaks are typical of tectosilicate structure (Freeman et al., 2008) and matched with those of Mexican and Chinese alkali feldspar specimens. However, the 455 cm^{-1} peak that appeared in orthoclase and microcline (Freeman et al., 2008) was absent in the Vietnamese anorthoclase. According to Bendel and Schmidt (2008), the increase in peak intensities at 165 and 474 cm^{-1} coupled with the decrease at 120 and 450 cm^{-1} corresponds to the transition from sanidine to anorthoclase. In addition to these features, the mole percent K/(Na+K) of alkali feldspar ranged between 0.11 and 0.38, representing a shift from monoclinic to triclinic crystal structure and thus indicating anorthoclase rather than sanidine. The 510 cm^{-1} band was attributed to a mixed Si-O-Si (or Si-O-Al) bending/stretching mode (Mernagh, 1991). The absence of the 450 cm^{-1} peak points to anorthoclase rather than microcline and orthoclase, in which the peak is present (Mernagh, 1991).

Figure 8. Raman spectra of anorthoclase samples from southeast Vietnam include peaks at 165, 283, 476, and 510 cm^{-1} corresponding to alkali feldspar (Freeman et al., 2008). The absence of the 450 cm^{-1} peak with the mole percent K/(Na+K) ranging between 0.11 and 0.38 indicates the anorthoclase variety.

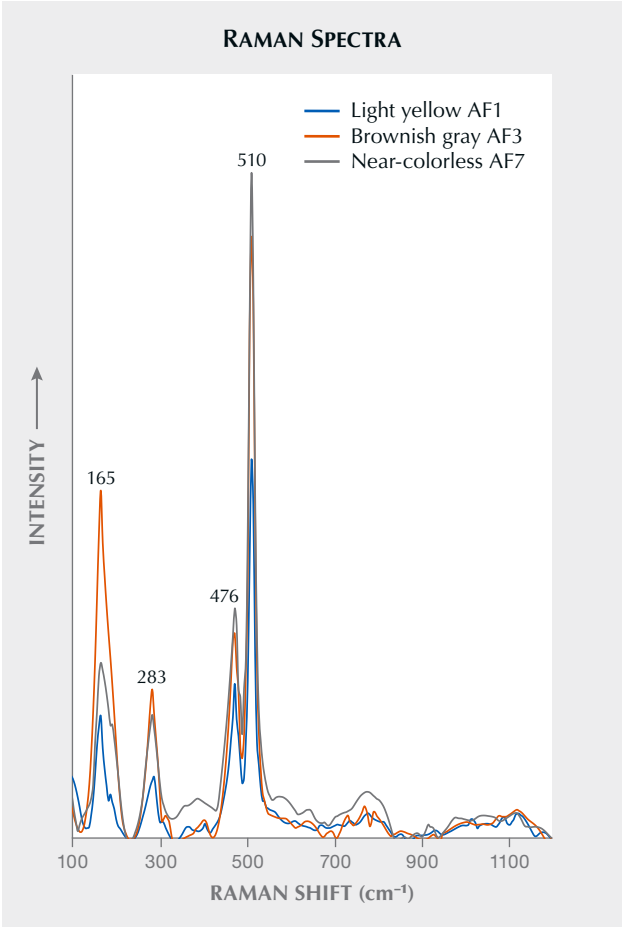

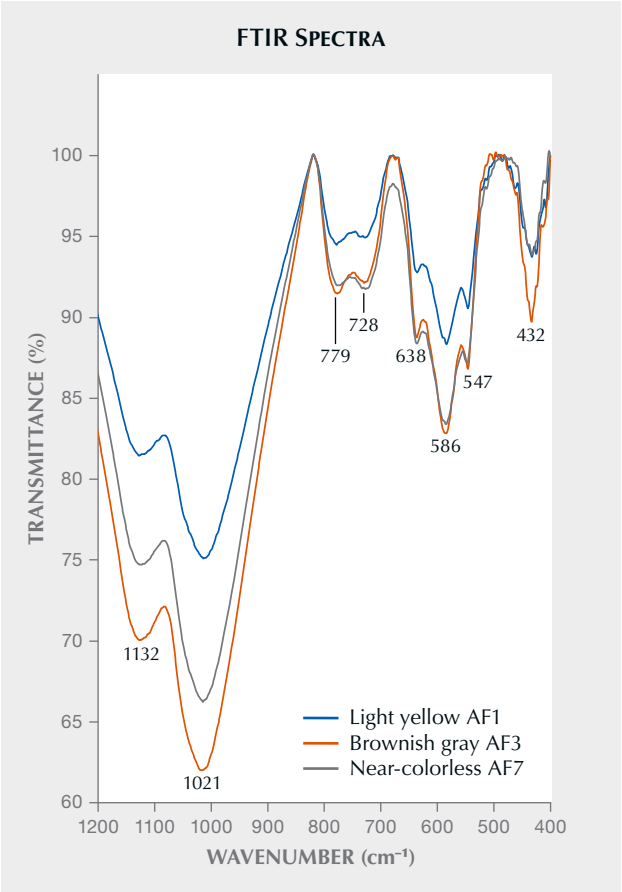

Figure 9. FTIR spectra of anorthoclase samples from southeast Vietnam indicate feldspar but cannot classify the anorthoclase variety. Note that transmittance mode was used due to the high scattering of samples.

Infrared Spectroscopy. The FTIR spectra of samples AF1, AF3, and AF7 (figure 9) showed relatively similar absorption bands in the 1200–400 cm^{-1} range, including 1132, 1021, 779, 728, 638, 586, 547, and 432 cm^{-1}. The 432 cm^{-1} peak was related to Si-O-Si deformation. The 547 cm^{-1} peak was associated with O-Si-O bending and M-O stretching (where M is the metal iron, magnesium, or manganese substituting for silicon). Peaks at 586 and 638 cm^{-1} were attributed to O-Si(Al)-O bending. Meanwhile, the 728 cm^{-1} peak corre-

Figure 10. A large anorthoclase mass (7.1 × 6 9 × 3.0 cm) weighing 1550 ct was cut in half, and the two pieces are shown in these photos. The opaque section on the left is suitable for a cabochon, while the more transparent section on the right could be used for faceting. Photos by Le Ngoc Nang.

sponded to Si-Al(Si) stretching and the 779 cm^{-1} peak to Si-Si stretching. Peaks at 1021 and 1132 cm^{-1} indicated Si-O stretching and Si(Al)-O stretching, respectively (Zhang et al., 1996). Hence, the infrared spectra of feldspar from southeast Vietnam are also typical of both sodium-rich and potassium-rich feldspars (Bosch-Reig et al., 2017), and therefore they are not useful for distinguishing anorthoclase from other feldspars.

GEM QUALITY AND POTENTIAL JEWELRY APPLICATION

Gem and non-gem anorthoclase have been reported from several locations, including Australia (Bahat, 1979), Portugal (Zanon et al., 2013), Antarctica (Sun and Hanson, 1976), the United States (Irving and Frey, 1984), and Cuba (Yin and Dai, 2021). It has not traditionally been used in jewelry because of its low transparency and easily split cleavages. Anorthoclase is rarely mentioned as a gem material, partly because it is mistaken for other alkali feldspars such as orthoclase or sanidine due to their similar appearance and gemological properties. This confusion could contribute to its unfamiliarity among many gem dealers.

Nang and Tien (2021) previously evaluated anorthoclase from southeast Vietnam for its color, transparency, stability to cutting and polishing, and chatoyant phenomenon. All three hues were appropriate for jewelry making, but yellow is traditionally a favorite color in the gem markets of Ho Chi Minh City (the same is true for other gem species such as sapphire and quartz). Some 70% of the anorthoclase collected was transparent. We also obtained several semitransparent samples, while the rest were translucent to opaque. The sizes were relatively large, usually around 15 ct up to more than 1500 ct (10–50 mm in size). High-quality anorthoclase is suitable for faceting into gems (again, see figures 1–4 and figure 11), while less-transparent material is more suitable for cutting into cabochons. Only 8% of the samples could be faceted to produce stones larger than 1 ct. More than 30% of the samples, which included the largest crystal at a weight of 1550 ct (figure 10), were suitable for cabochons. In the study group, the largest facet-quality rough anorthoclase was 144.80 ct (AF11), and the largest faceted stone to date was sample AF1, which weighed 25.99 ct and was mounted as a pendant (figure 11).

The samples had a Mohs hardness of 6.0–6.5, indicating moderate durability. However, perfect cleavage and multiple albite-law twinning planes in anorthoclase make gem manufacturing difficult and require extra care during use.

Low-quality feldspar can be treated to enhance its color, durability, and clarity. Examples include impregnating moonstone and amazonite with plastic to improve transparency (Jianjun et al., 2013; Sun and Renfro, 2017) and diffusing copper to create red labradorite imitations of andesine (Zhou et al., 2022). Anorthoclase from Dong Nai is still too novel for any known treatment practices. But it is a promising candidate for treatment, given the abundance of samples in the area.

Figure 11. This 25.99 ct light yellow anorthoclase (sample AF1) is set in a 14K gold pendant. Photo by Le Ngoc Nang.

The anorthoclase-bearing basalt and its weathering products cover approximately 1000 km^2 in southeast Vietnam, with depths of 30 to 100 m (Tich et al., 2004). Its weathering products, which range from 1 to 3 m in thickness, are a rich source of anorthoclase. On average, a cubic meter of basaltic material might contain three to five anorthoclase crystals, while the concentration is higher in weathering products because the gems are released from the bedrock by erosion and accumulated along the hill slopes. In Dong Nai, the weathering products are easily accessible by dirt roads surrounded by arable lands.

The gem quality, distribution, and mining feasibility of anorthoclase from southeast Vietnam suggests a potentially valuable deposit. In addition, the locality could become a geotourism attraction with basalt-related gemstones across the region.

CONCLUSIONS

Anorthoclase from Dong Nai Province in southeast Vietnam presents as transparent to translucent crystals that are brownish gray, yellow, and near-colorless. It is not practical to distinguish feldspar varieties using only standard gemological methods. The composition determined for the samples was $An_{3.50–8.02}$, $Ab_{58.83–81.69}$, and $Or_{11.94–36.96}$, which falls within the anorthoclase field on the An–Ab–Or ternary diagram. Interpretation of XRD results firmly concluded the anorthoclase variety. The Raman and FTIR spectra of anorthoclase from southeast Vietnam are similar to those from other regions in the world. Vietnamese anorthoclase has commercial potential, as there are significant amounts of gem-quality material suitable for faceting and cutting into cabochons. Lastly, these materials have a widespread distribution across the region, with a high concentration in the basaltic weathering products.

ABOUT THE AUTHORS

Le Ngoc Nang is a postgraduate in the geology faculty at the University of Science, Vietnam National University in Ho Chi Minh City, and CEO of Liu Gemological Research and Application Center (LIULAB), where Pham Minh Tien is a technical specialist. Pham Minh is a lecturer, and Dr. Pham Trung Hieu is an associate professor, in the geology faculty at the University of Science, Vietnam National University.

ACKNOWLEDGMENTS

We express gratitude to Tran Ngoc Vien for leading us to the sampling areas during our field trips to Dong Nai. This research was funded by the National Foundation for Sciences and Technology Development of Vietnam (NAFOSTED) under grant number 105.01-2021.18.

REFERENCES

Anthony J.W., et al. (2001) Anorthoclase. In *Handbook of Mineralogy*, Mineralogical Society of America, Chantilly, Virginia.

Bahat D. (1979) Anorthoclase megacrysts: Physical conditions of formation. *Mineralogical Magazine*, Vol. 43, No. 326, pp. 287–291, http://dx.doi.org/10.1180/minmag.1979.043.326.11

Barr S.M., MacDonald A.S. (1981) Geochemistry and geochronology of late Cenozoic basalts of Southeast Asia. *Geological Society of America Bulletin*, Vol. 92, No. 8 (part II), pp. 1069–1142, http://dx.doi.org/10.1130/GSAB-P2-92-1069

Bendel V., Schmidt B.C. (2008) Raman spectroscopic characterisation of disordered alkali feldspars along the join $AlSi_3O_8$–$NaAlSi_3O_8$: Application to natural sanidine and anorthoclase. *European Journal of Mineralogy*, Vol. 20, No. 6, pp. 1055–1065, http://dx.doi.org/10.1127/0935-1221/2009/0021-1856

Bonewitz R.L. (2008) *Rock and Gem: The Definitive Guide to Rocks, Minerals, Gemstones, and Fossils*. DK Publishing, New York.

Bosch-Reig F., Gimeno-Adelantado J.V., et al. (2017) Quantification of minerals from ATR-FTIR spectra with spectral interferences using the MRC method. *Spectrochimica Acta Part A*, Vol. 181, pp. 7–12, http://dx.doi.org/10.1016/j.saa.2017.02.012

Carter A., Roques D., et al. (2001) Understanding Mesozoic accretion in Southeast Asia: Significance of Triassic thermotectonism (Indosinian orogeny) in Vietnam. *Geology*, Vol. 29, No. 3, pp. 211–214, http://dx.doi.org/10.1130/0091-7613(2001)029%3C0211:UMAISA%3E2.0.CO;2

Clift P.D., Carter A., et al. (2002) Constraints of India–Eurasia collision in the Arabian Sea region taken from the Indus Group, Ladakh Himalaya, India. *Geological Society, London, Special Publications*, Vol. 195, pp. 97–116, http://dx.doi.org/10.1144/GSL.SP.2002.195.01.07

Deer W.A., Howie R.A., Zussman J. (2001) *Rock-Forming Minerals*, 2nd ed., Volume 4A. The Geological Society, London.

Freeman J.J., Wang A., et al. (2008) Characterization of natural feldspars by Raman spectroscopy for future planetary exploration. *Canadian Mineralogist*, Vol. 46, No. 6, pp. 1477–1500, http://dx.doi.org/10.3749/canmin.46.6.1477

Glascock M.D. (2020) Tables to support the analytical methods in use at MURR: NAA, XRF, and ICP-MS. University of Missouri Research Reactor (MURR), Columbia.

Gübelin E.J., Koivula J.I. (2005) *Photoatlas of Inclusions in Gemstones, Volume 2*. Opinio Publishers, Basel, Switzerland.

Harlow G.E. (1982) The anorthoclase structures: The effects of temperature and composition. *American Mineralogist*, Vol. 67, No. 9-10, pp. 975–996.

Hoang N., Flower M.F.J. (1998) Petrogenesis of Cenozoic basalts from Vietnam: Implication for origins of a "diffuse igneous province." *Journal of Petrology*, Vol. 39, No. 3, pp. 369–395, http://dx.doi.org/10.1093/petroj/39.3.369

Hoang N., Flower M.F.J., Carlson R.W. (1996) Major, trace element, and isotopic compositions of Vietnamese basalts: Interaction of hydrous EM1-rich asthenosphere with thinned Eurasian lithosphere. *Geochimica et Cosmochimica Acta*, Vol. 60, No. 22, pp. 4329–4351, http://dx.doi.org/10.1016/S0016-7037(96)00247-5

Irving A.J., Frey F.A. (1984) Trace element abundances in megacrysts and their host basalts: Constraints on partition coefficients and megacryst genesis. *Geochimica et Cosmochimica Acta*, Vol. 48, pp. 1201–1221, http://dx.doi.org/10.1016/0016-7037(84)90056-5

Jianjun L., Xiaofan W., et al. (2013) Infrared spectroscopic study of filled moonstone. *G&G*, Vol. 49, No. 1, pp. 28–34, http://dx.doi.org/10.5741/GEMS.49.1.28

Jones J.B., Taylor W.H. (1961) The structure of orthoclase. *Acta Crystallographica*, Vol. 14, No. 5, pp. 443–456, http://dx.doi.org/10.1107/S0365110X61001479

Leech M.L., Singh S., et al. (2005) The onset of India–Asia continental collision: Early, steep subduction required by the timing of UHP metamorphism in the western Himalaya. *Earth and Planetary Science Letters*, Vol. 234, No. 1-2, pp. 83–97, http://dx.doi.org/10.1016/j.epsl.2005.02.038

Lepvrier C., Vuong N.V., et al. (2008) Indosinian tectonics in Vietnam. *Comptes Rendus Geoscience*, Vol. 340, No. 2-3, pp. 94–111, http://dx.doi.org/10.1016/j.crte.2007.10.005

Levin I. (2018) NIST Inorganic Crystal Structure Database (ICSD). National Institute of Standards and Technology, http://dx.doi.org/10.18434/M32147

Mernagh T.P. (1991) Use of the laser Raman microprobe for discrimination amongst feldspar minerals. *Journal of Raman Spectroscopy*, Vol. 22, No. 8, pp. 453–457, http://dx.doi.org/10.1002/jrs.1250220806

Morrison N., Cox R. (2014) An investigation into UV fluorescence in feldspar group minerals. *Atlantic Geology*, Vol. 50, No. 1, pp. 24–35.

Nang L.N., Tien P.M. (2021) Chatoyant anorthoclase feldspar from Dong Nai Province, Vietnam. *Journal of Gemmology*, Vol. 37, No. 7, pp. 672–673.

Rangin C., Klein M., et al. (1995) The Red River fault system in the Tonkin Gulf, Vietnam. *Tectonophysics*, Vol. 243, No. 3-4, pp. 209–222, http://dx.doi.org/10.1016/0040-1951(94)00207-P

Smith J.V., Brown W.L. (1988) *Feldspar Minerals*, 2nd ed. Springer-Verlag, Berlin.

Son N.D., Du D.C., et al. (2005) Geological mapping of mineral resource and prospective zoning of Dong Nai Province, scale 1:50.000, Dong Nai Department of Science and Technology.

Sun S.S., Hanson G.N. (1976) Rare earth element evidence for differentiation of McMurdo volcanics, Ross Island, Antarctica. *Contributions to Mineralogy and Petrology*, Vol. 54, pp. 139–155, http://dx.doi.org/10.1007/BF00372120

Sun Z., Renfro N.D. (2017) Gem News International: Impregnated amazonite. *G&G*, Vol. 53, No. 3, pp. 384–385.

Tich P.X., Hoang N., Lee H.K. (2004) Geochemistry of late Cenozoic basalts in Vietnam and its tectonic significances. *Journal of Geology, Series B*, No. 24, pp. 65–76 [in Vietnamese].

Yin F., Dai D. (2021) Petrology and mineralogy of the Viñales meteorite, the latest fall in Cuba. *Science Progress*, Vol. 104, No. 2, http://dx.doi.org/10.1177/00368504211019859

Zanon V., Kueppers U., et al. (2013) Volcanism from fissure zones and the Caldeira central volcano of Faial Island, Azores archipelago: Geochemical processes in multiple feeding systems. *Geological Magazine*, Vol. 150, No. 3, pp. 536–555, http://dx.doi.org/10.1017/S0016756812000702

Zhang M., Wruck B., et al. (1996) Phonon spectra of alkali feldspars: Phase transitions and solid solutions. *American Mineralogist*, Vol. 81, No. 1-2, pp. 92–104, http://dx.doi.org/10.2138/am-1996-1-212

Zhou Q., Wang C., Shen A.H. (2022) Fluorescence characteristics of two copper-diffused plagioclase feldspars: Labradorite and andesine. *G&G*, Vol. 58, No. 4, pp. 424–437, http://dx.doi.org/10.5741/GEMS.58.4.424